Supporting Information

A Colorimetric Sensing Platform Based on Self-assembled 3D Porous CeGONRs Nanozymes for Label-Free Visual Detection of Organophosphate Pesticides

Liyun Lin, *[a] Huifang Ma, [a] Chunliang Yang, [a] Wuhai Chen, [a] Shaodong Zeng, *[a] and Yuefang Hu [b]

[a] Products Processing Research Institute, Chinese Academy of Tropical Agricultural Sciences, Zhanjiang 524001, Guangdong, China

[b] College of Materials and Chemical engineering, Hezhou University, Hezhou 542899, Guangxi, China

*Corresponding author:

liyyunlin@163.com (L. Lin)

shaodongzeng@163.com (S. Zeng)

1. Supporting experimental steps

1.1 Preparation of GONRs

GONRs were prepared using a previously published protocol with minor modifications. Briefly, SWCNTs (20.0 mg) were dispersed in concentrated sulfuric acid (H_2SO_4, 80 mL, 25% by volume) and mildly sonicated for 15 min, then treated with potassium permanganate ($KMnO_4$, 100 mg, 500 wt% by quality) and sonicated for another 15 min. The reaction mixture was stirred at room temperature for 1 h and then heated to 55-70°C for an additional 1 h. The acidic conditions are necessary for

longitudinal unzipping of SWCNTs. When the solution turned brown, heating stopped, and the solution was cooled. We examined the reaction by placing a few drops of the reaction solution into 1.0 mL of water (containing four drops of H_2O_2), there was no black granular residue, indicating that the reaction was complete. We then quenched the reaction mixture by pouring in 400 mL of ice water containing 2.0 mL of H_2O_2 concentrate into the solution. The acquired solution was filtered over a polytetrafluoroethylene (PTFE) membrane and the remaining solid was washed with water several times. The sample was dialyzed for 24 h and the solid was collected for analysis.

1.2 Enzyme kinetics experiments

The catalytic activity of the CeGONRs was evaluated by enzyme kinetics theory and methods. Kinetic measurements were conducted in time course mode by monitoring the absorption intensity at 654 nm. Kinetic experiments were manipulated using 6.67 μg/mL CeGONRs in a reaction volume of 2.2 mL NaAc buffer (0.2 M, pH 4.0) within a range of substrate concentrations (TMB). The Michaelis–Menten constant (K_m) was calculated using the double reciprocal of the Michaelis–Menten equation: $1/v=(K_m/V_{max}).(C + 1/V_{max})$, where v is the initial velocity, V_{max} is the maximal reaction velocity, and C is the substrate concentration.

1.3 Detection of chlorpyrifos in cabbage samples

Detection of chlorpyrifos in cabbage samples bought from the local Wal-Mart supermarket were chosen to test the feasibility of our method. First, the cabbages were cut into pieces and stirred. Next, 40.0 mL of acetonitrile was added into 20.0 g of sample and stirred for 30 min. Then the mixture was filtered, and the residue was washed again with acetonitrile. The filtrate was combined with NaCl solution, shaken for 3 min and allowed to stand for 1 h. After drying under nitrogen, the solvent was removed. Finally, the settled solids were dissolved and the prepared samples were stored at 4°C.

The residual amount of CP was determined using the accepted method of HPLC-MS to examine the accuracy of the established method. The cabbage samples were divided into four parts (A, B, C, D, respectively) of 200.0 g each, and a dose of chlorpyrifos (60.0 μg kg^{-1}) was sprayed on B, C, D cabbage samples. After standing for 12 h, the samples were processed according to the above steps. Then the sample was measured by HPLC-MS. Chromatographic conditions were as follows: column, UPLC ACQUITY BEH, 50×2.1 mm, 1.7 μm; mobile phase acetonitrile (A)/0.1 aqueous formic acid (V: V); gradient elution, 0-1 min, 90% A; 1-2.2 min, 90% A-50% A; 2.2-3 min, 50%-90% A; 3-4 min, and 90% A for 1 min. Mass spectrometry conditions: ion source ESI, positive ion; ion source temperature 110 °C; and monitored ion pair: 349/97, 349/198.

1.4 The fabricated of test strips

The test strips were fabricated for OP detection. Briefly, 90 μL of the supernatant from step 2.4 was dropped on the paper, 30 μL of chlorpyrifos solutions at different concentrations (0.012, 0.10, 0.50, 1.0, 1.5, 2.0, 2.5, 3.0, 3.5) were mixed with 30 μL of AChE solution (1.0 U mL^{-1}), then 30 μL ATCh solution (10 mM) and 150 μL PBS buffer (10 mM, pH 7.5) was added and mixed thoroughly then dropped on the paper.

2. Supporting Figures

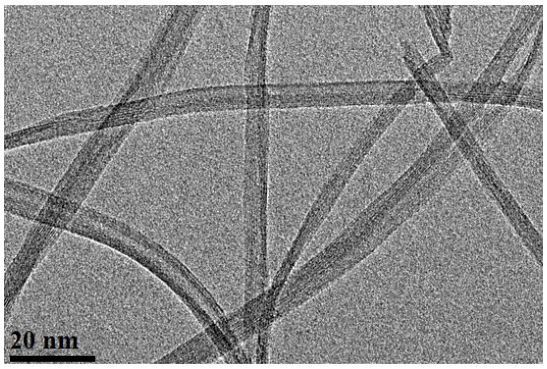

Fig. S1 TEM images of the obtained GONRs.

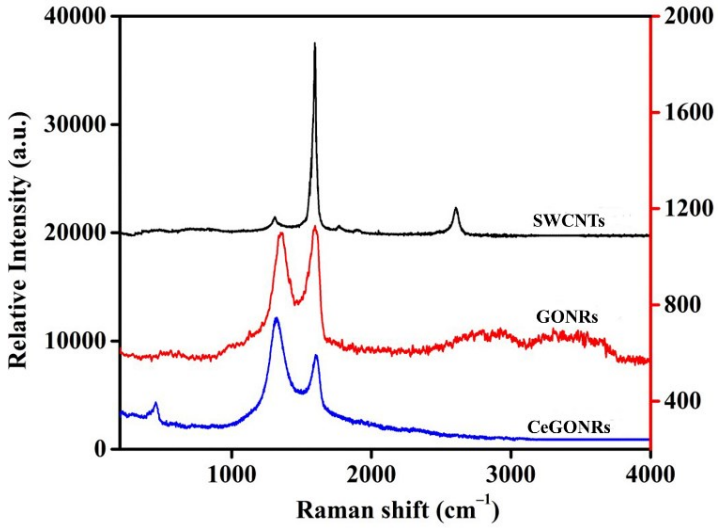

Fig. S2 Raman spectroscopy of SWCNTs, GONRs, and CeGONRs.

Raman spectroscopy (Fig. S2) was conducted to explore SWCNTs, GONRs, and CeGONRs, which exhibited a peak at 1305 cm^{-1} (called the D-band) and first-order scattering of the E2g phonons at 1593 cm^{-1} (G-band)[1]. The intensity ratio (D/G) of the D- and G-band of GONRs was enhanced after oxidation [2]. This confirmed a marked increase in the degree of disorder and defective sites on the GONRs. These defective sites were beneficial for anchoring nanoceria to the support surface. The epoxy C-O oxidized the mobility of Ce(III) and the two bands shifted to 1322 and 1598 cm^{-1}, revealing a charge transfer between the GONRs and nanoceria[3]. Another peak was observed at 490 cm^{-1}, which was assigned Ce-O vibrations [4]. The appearance of the D-band at 1358 cm^{-1}, attributed to GONRs, also predicted the degree of defect of

the sample (which, again, was beneficial to nanoceria precipitation). Simultaneously, the precipitated nanoceria on the GONRs further enhanced the D-band at 1358 cm^{-1} and facilitated substrate adsorption on the defect surface.

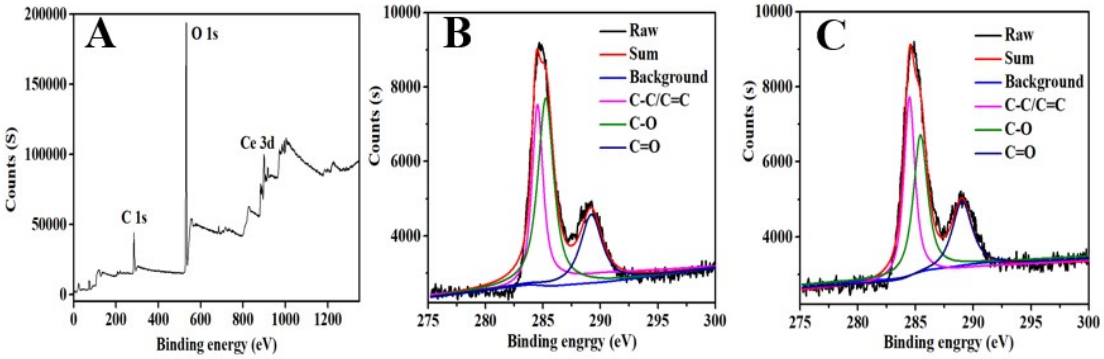

Fig. S3 The XPS survey spectrum of CeGONRs (A), C 1s spectrum of GONRs (B), and CeGONRs (C).

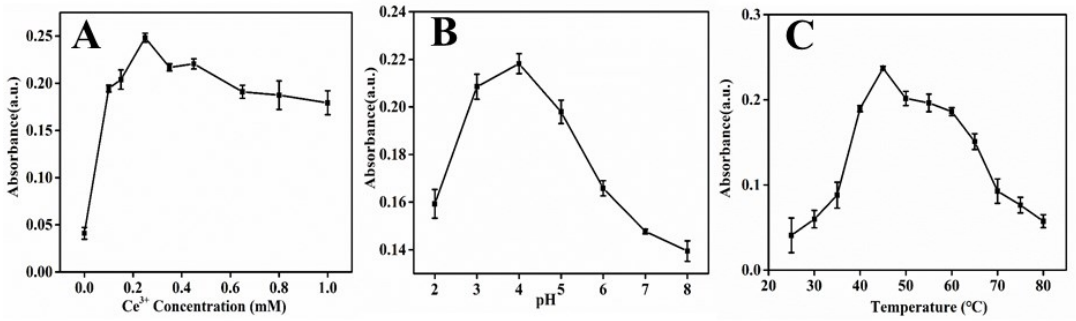

Fig. S4 The catalytic activities of CeGONRs with different Ce^{3+} concentrations (A). The catalytic activities of CeGONRs at different pH (B), and temperature (C).

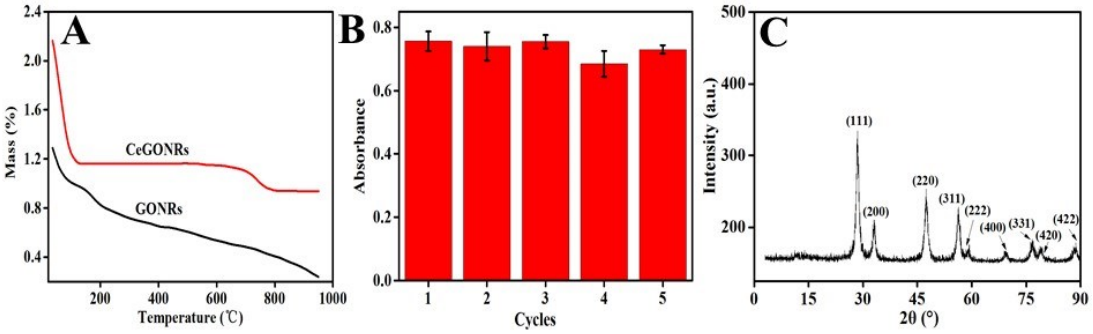

Fig. S5 (A) The thermogravimetric analysis (TGA) results. (B) Five consecutive catalysis cycles of CeGONRs. (C) The XRD of recycling products CeGONRs for five catalytic reactions.

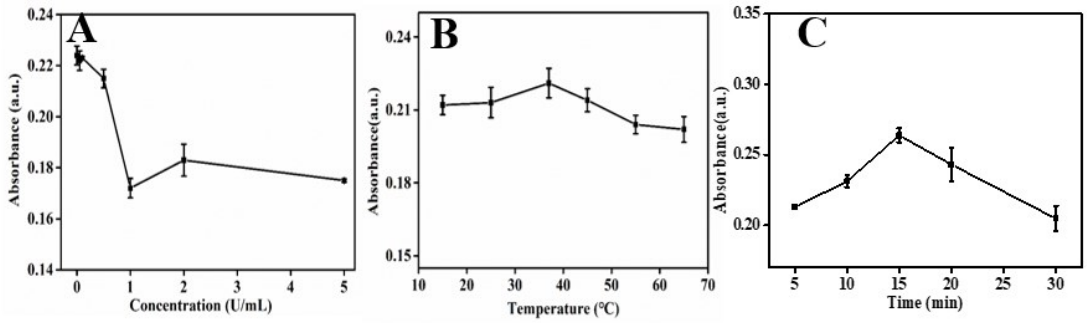

Fig. S6 The effect of AChE concentrations (A), temperature (B), and time (C), on the catalytic activity of CeGONRs. The experiments were repeated three times.

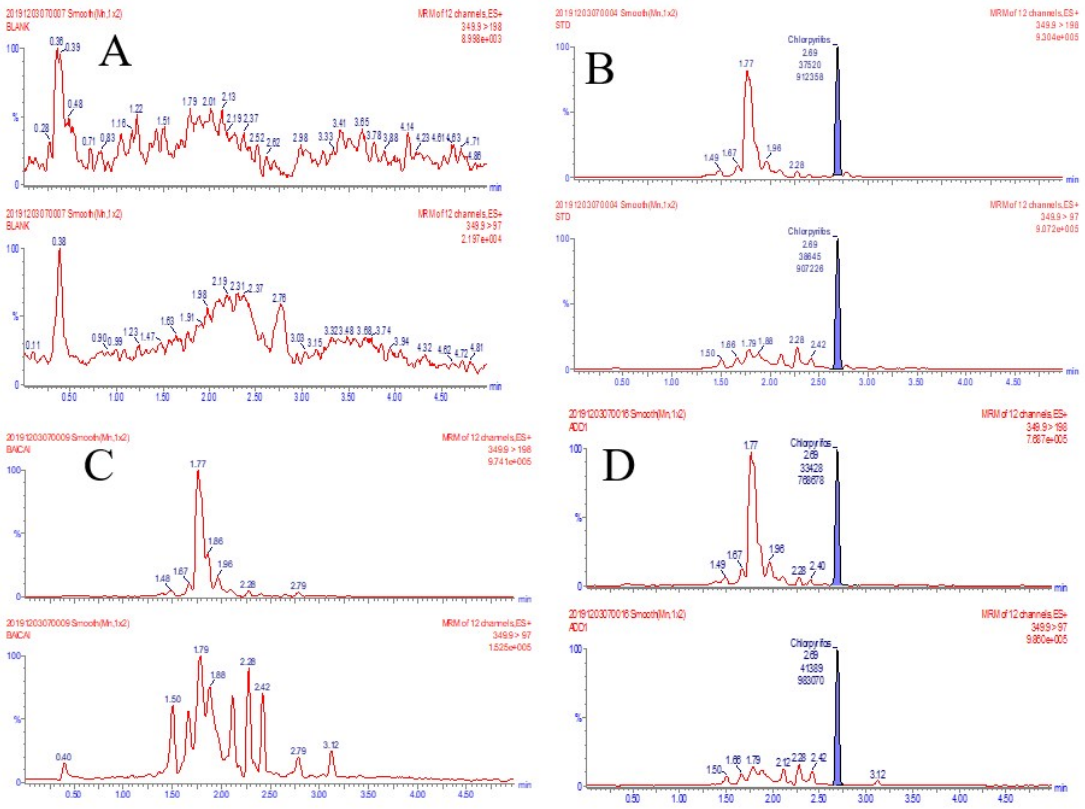

Fig. S7 Determination of chlorpyrifos content in cabbage samples by liquid chromatography-mass spectrometry, reagent blank(A), matrix preparation standard solution (B), the cabbage sample (C) and cabbage samples sprayed with 60.0 μg/kg chlorpyrifos(D).

3. Supporting Table

Table S1 Comparison of the apparent Michaelis–Menten constant (K_m) and maximum reaction rate (V_{max}) for CeO_2 NPs, CeGONRs and HRP.

Catalyst	Substance	K_m [μM]	V_{max} [10^{-8} Ms^{-1}]	References
HRP	TMB	275	1.24	[5]
CeO_2 NPs	TMB	269	1.14	[6]
CeGONRs	TMB	0.109	6.08	This work

Table S2. The comparison of different methods for detecting organophosphorus pesticides.

Materials	OPs	Methods	Linear range	Detection Limit	References
CeGONRs	Chlorpyrifos	Colorimetric	0.012-3.5 μg mL^{-1}	3.43 ng mL^{-1}	This work
GO	Chlorpyrifos	Colorimetric	0.002-0.1 μg mL^{-1}	2 ng mL^{-1}	[7]
CS@TiO_2-CS/rGO	Dichlorvos	Electrochemical	0.036-22.6 μM	29 nM	[8]
Au NCs	Chlorpyrifos	Luminescent	0-5.0 μM	0.5 μM	[9]
EuMOFs/CDs@CMC	Chlorpyrifos	Fluorescent	5-40 μM	89 nM	[10]
SPE/PHA/ mPEG	Chlorpyrifos	Electrochemical	1.0-10.0 μM	0.83μM	[11]
AuNRs@MS	Dichlorvos	Electrochemical	0.18-13.6 μM	5.3 nM	[12]
	Fenthion			1.3 nM	
MnOOH NWs	Omethoate	Electrochemical	5-50 ng mL^{-1}	0.35 ng mL^{-1}	[13]
	Dichlorvos		1-10 ng mL^{-1}	0.14 ng mL^{-1}	
TiO_2 NPs	Methyl paraoxon	Electrochemical	0.5–100 μM	0.24 μM	[14]
	Methyl parathion			0.22 μM	
AIEgens-SiO_2-MnO_2	Paraoxon	Fluorescent	1–100 μg L^{-1}	1 μg L^{-1}	[15]
QDs	Parathionparaoxon	Fluorescent	5-100 mg L^{-1}	10 μg mL^{-1}	[16]
AuPt Hydrogels	paraoxon-ethyl	Electrochemical	0.5-1000 ng L^{-1}	0.185 ng L^{-1}	[17]

Table S3 Standard addition method utilized for quantitative analyses of chlorpyrifos in cabbage samples, and results of the recovery experiment

Sample	Added (μg kg^{-1})	Found (μg kg^{-1})	Recovery (%)	RSD (%)
1	0	0	—	—
2	60.0	62.7	104.5	3.1
3	100.0	103.0	103.0	2.9
4	200.0	191.4	95.7	2.3

References

[1] Song Y, Qu K, Zhao C, et al. Advanced Materials, 2010, 22(19): 2206-2210.

[2] Sun L, Ding Y, Jiang Y, et al. Sensors and Actuators B: Chemical, 2017, 239: 848-856.

[3] Fu L, Wang Y, Zhang K, et al. ACS nano, 2019, 13(6): 6341-6347.

[4] Jiao L, Zhang L, Wang X, et al. Nature, 2009, 458(7240): 877.

[5] Kosynkin D V, Higginbotham A L, Sinitskii A, et al. Nature, 2009, 458(7240): 872.

[6] Jiang S, Hou P X, Chen M L, et al.. Science advances, 2018, 4(5): eaap9264.

[7] Chu S, Huang W, Shen F, et al. Nanoscale, 2020.(DOI: 10.1039/C9NR10862A)

[8] Cui H F, Wu W W, Li M M, et al. Biosensors and Bioelectronics, 2018, 99: 223-229.

[9] Lu Q, Zhou T, Wang Y, et al. Biosensors and Bioelectronics, 2018, 99: 274-280.

[10] Xu X Y, Yan B, Lian X. Nanoscale, 2018, 10(28): 13722-13729.

[11] Sgobbi L F, Machado S A S. Biosensors and Bioelectronics, 2018, 100: 290-297.

[12] Cui H F, Zhang T T, Lv Q Y, et al. Biosensors and Bioelectronics, 2019, 141: 111452.

[13] Huang L, Sun D W, Pu H, et al. Sensors and Actuators B: Chemical, 2019, 290: 573-580.

[14] Qiu L, Lv P, Zhao C, et al. Sensors and Actuators B: Chemical, 2019, 286: 386-393.

[15] Wu X, Wang P, Hou S, et al. Talanta, 2019, 198: 8-14.

[16] Luan E, Zheng Z, Li X, et al. Analytica Chimica Acta, 2016, 916: 77-83.

[17] Wu Y, Jiao L, Xu W, et al. Small, 2019, 15(17): 1900632.